

τ -lepton pair spin in proton-proton LHC collisions for anomalous dipole moments

A.Yu. Korchin^{a,b,c}, E. Richter-Was^c, Yu. Volkotrub^c and Z. Was^d

^a*NSC Kharkiv Institute of Physics and Technology, 61108 Kharkiv, Ukraine*

^b*V.N. Karazin Kharkiv National University, 61022 Kharkiv, Ukraine*

^c*Institute of Physics, Jagiellonian University, ul. Lojasiewicza 11, 30-348 Krakow, Poland*

^d*Institute of Nuclear Physics Polish Academy of Sciences, PL-31342 Krakow, Poland*

ABSTRACT

The spin correlations in the pair of τ leptons produced in the high-energy proton-proton collisions are studied. The invariant mass of the τ -lepton pair is chosen close to Z -boson mass, in these conditions Z -boson exchange gives the dominant contribution to the Drell-Yan mechanism. The interaction of Z boson with τ lepton, in addition to the Standard Model couplings, can include weak anomalous magnetic and electric dipole moments (or form-factors) of the τ lepton. Dependence of elements of the pp spin-correlation matrix on the weak anomalous moments is determined for various regions of the rapidity of the τ -lepton pair. Based on this calculation, we construct a semi-realistic observable built on the momenta of pions in the $\tau^\mp \rightarrow \pi^\mp \nu_\tau$ and $\tau^\pm \rightarrow \rho^\pm \nu_\tau \rightarrow \pi^\pm \pi^0 \nu_\tau$ decay channels, and show that this observable can be sensitive to the weak anomalous dipole moments.

1 Introduction

One of the interesting topics of present-day phenomenology relates to measurement or establishing limits on the muon anomalous dipole moments, magnetic and electric ones. Numerous papers were devoted to that subject (see [1, 2] and references therein), and experimental measurements [3, 4, 5] may indicate that deviation of the measured value of anomalous magnetic moment from the Standard Model (SM) prediction is at the edge of the discovery. Independently, if this is the case, one should prepare alternative or supplementary measurements and necessary for their interpretation calculations and software tools.

The production and decay of τ -lepton pair offer interesting research direction, because anomalous magnetic dipole moments due to possibly enhanced contributions from New Physics (NP) models are expected to be proportional to the mass squared of the lepton, and are therefore enhanced for the τ lepton by a factor of 280 compared to the muon. This makes these studies important and of contemporary interest.

The LHC experiments [6, 7, 8], taking data now, offer immediate opportunity for the measurements. The τ lepton decays and the τ -decay products are observed and provide access to the physics information embedded in the τ -lepton pair spin state. Neither incoming partons in the hard scattering process nor all τ -decay products (due to neutrinos escaping detection) are available for direct measurement. To simplify the task of observable build and of measurement interpretation, tools like `TauSpinner` [9, 10, 11] can be helpful. Since Ref. [12], the tool can be used to calculate event weights introducing anomalous dipole moments.

However, these papers do not address the actual impact of dipole moments on τ -decay products distributions. In the present paper, we address the topic in the context of the pp collisions in the conditions of the LHC, which was not covered previously. The consideration is focused on the region of τ -pair invariant mass around Z -boson mass. In these conditions, the Z -boson exchange mechanism of the Drell-Yan production of the τ pair is the dominant one, and the coupling of Z boson to τ leptons may carry information on weak anomalous magnetic and/or electric dipole moments of the τ lepton.

In Section 2 we describe differential cross section in terms of the spin-correlation matrix in the high-energy proton-proton collisions. In Section 3 some results for elements of effective proton-proton spin-correlation matrix are presented in different kinematical regimes. Section 4 is devoted to the definition of a prototype observable that is sensitive to weak anomalous dipole moments. It is distinct from the one used in `TauSpinner` algorithm because it relies on detectable momenta only; it does not use the momenta of τ leptons. Conclusions are given in Section 5.

2 Differential cross section of $p + p \rightarrow Z + \dots \rightarrow \tau^- + \tau^+ + \dots$

In this section, we present a differential cross section of the reaction $p + p \rightarrow Z + \dots \rightarrow \tau^- + \tau^+ + \dots$ as a function of the τ -lepton rapidities y_- , y_+ and τ -pair invariant mass (squared) $M^2 = (p_- + p_+)^2 = x_1 x_2 s$, where s is invariant energy squared in the pp collision. Here x_1 and x_2 are fractions of the proton momenta p_1 and p_2 carried by partons f and \bar{f} , respectively.

The differential cross section of the process $p + p \rightarrow \tau^- + \tau^+ + \dots$ is written as (see, e.g. [13], Ch. 17.4)

$$\frac{d\sigma}{dx_1 dx_2 dt}(pp \rightarrow \tau^- \tau^+ + \dots) = \sum_{f=q,\bar{q}} F_f(x_1) F_{\bar{f}}(x_2) \frac{d\sigma}{dt}(f\bar{f} \rightarrow \tau^- \tau^+), \quad (1)$$

where $F_f, \bar{f}(x)$ are the parton distribution functions (PDF)s, which also depend on an energy scale Q (not indicated explicitly).

The total four-momentum of the τ pair in the parton-parton process $f(x_1 p_1) + \bar{f}(x_2 p_2) \rightarrow \tau^-(p_-) + \tau^+(p_+)$ is

$$\begin{aligned} q^\mu &= (q^0, \vec{q}), & \vec{q} &= (0, 0, q), \\ q^0 &= E_- + E_+ = \frac{\sqrt{s}}{2} (x_1 + x_2), & q &= p_{-\parallel} + p_{+\parallel} = \frac{\sqrt{s}}{2} (x_1 - x_2). \end{aligned} \quad (2)$$

Hereafter the mass of the proton is neglected. The fractions of the proton momenta

$$x_1 = \frac{M}{\sqrt{s}} \exp(Y_Z), \quad x_2 = \frac{M}{\sqrt{s}} \exp(-Y_Z) \quad (3)$$

are expressed through the invariant mass and rapidity of the τ pair

$$Y_Z = \ln \left(\frac{q^0 + q}{M} \right) = \frac{1}{2} \ln \left(\frac{x_1}{x_2} \right). \quad (4)$$

To include angular dependence of the hard process $f\bar{f} \rightarrow \tau^- \tau^+$ we introduce the longitudinal rapidities of τ^- and τ^+ via the relations [13]:

$$\begin{aligned} E_- &= p_\perp \cosh(y_-), & p_{-\parallel} &= p_\perp \sinh(y_-), & \vec{p}_{-\perp} &= \vec{n}_\perp p_\perp, \\ E_+ &= p_\perp \cosh(y_+), & p_{+\parallel} &= p_\perp \sinh(y_+), & \vec{p}_{+\perp} &= -\vec{n}_\perp p_\perp, \end{aligned} \quad (5)$$

where ‘‘parallel’’ (‘‘perpendicular’’) means longitudinal (transverse) to the beam components of the τ^\mp momenta, \vec{n}_\perp is the unit vector in the transverse direction, and we assume that initial partons do not have transverse momenta.

It is straightforward to relate rapidities of τ^- and τ^+ with the lepton pair rapidity Y_Z and variable y^* , which has the meaning of the τ^- rapidity in the center-of-mass (c.m.) frame of the $\tau^- \tau^+$ pair. Namely,

$$y_- = Y_Z + y^*, \quad y_+ = Y_Z - y^*. \quad (6)$$

The rapidity of τ^+ in the c.m. frame is $-y^{*1}$. Note that the c.m. angle θ^* between the parton f and τ^- is determined from

$$\sin \theta^* = \frac{1}{\cosh(y^*)}, \quad \cos \theta^* = \tanh(y^*). \quad (7)$$

The transverse momentum of τ 's is $p_\perp = \frac{1}{2}M \sin \theta^*$ and the invariant momentum transfer t of Eq. (1) is equal to $t = -\frac{1}{2}M^2(1 - \cos \theta^*)$.

We will choose the variables Y_Z, y^* , and M^2 as independent ones. Then the triply differential cross section can be written as

$$\begin{aligned} \frac{d\sigma}{dY_Z dy^* dM^2}(pp \rightarrow \tau^- \tau^+ + \dots) &= \frac{x_1 x_2}{2 \cosh^2(y^*)} \quad (8) \\ &\times \sum_{f=\bar{q}} F_f(x_1) F_{\bar{f}}(x_2) \frac{d\sigma}{dt}(f \bar{f} \rightarrow \tau^- \tau^+), \end{aligned}$$

where the factor $x_1 x_2$ originates from the Jacobian due to change of variables from (x_1, x_2, t) to (Y_Z, y^*, M^2) . The cross section of the quark-antiquark production of the polarized τ leptons is [12]

$$\frac{d\sigma}{dt}(q\bar{q} \rightarrow \tau^- \tau^+) = \frac{\beta}{16\pi M^4} \sum_{i,j=1}^4 R_{i,j}^{(q\bar{q})}(M, \theta^*) S_i^- S_j^+. \quad (9)$$

Here $S_i^\mp = (\vec{S}^\mp, 1)$ and \vec{S}^\mp are the polarization vectors of τ^\mp in their corresponding rest frames. The Cartesian components of vectors \vec{S}^\mp are defined in a system with the axes $(\hat{x}', \hat{y}', \hat{z}')$, where \hat{z}' is along the c.m. momentum of τ^- , plane $\hat{x}'\hat{z}'$ is spanned on the c.m. momenta of τ^- and q , and $\hat{y}' = \hat{z}' \times \hat{x}'$. The normalized spin-correlation matrix is expressed in terms of the coefficients $R_{i,j}^{(q\bar{q})}(M, \theta^*)$ as $r_{i,j}^{(q\bar{q})} \equiv R_{i,j}^{(q\bar{q})}/R_{44}^{(q\bar{q})}$. Besides, in Eq. (9) $\beta = (1 - 4m_\tau^2/M^2)^{1/2} \approx 1$ is the τ -lepton velocity in the c.m. frame.

2.1 Analysis of kinematics

A typical configuration of τ -lepton momenta in laboratory frame is shown in Fig. 1. Here α_+ and α_- are the angles of τ^+ and τ^- with respect to the proton beam axis. They are related to the corresponding rapidities

$$\cos \alpha_\pm = \frac{p_{\pm\parallel}}{E_\pm} = \tanh(y_\pm), \quad y_\pm = \tanh^{-1}(\cos \alpha_\pm) = \frac{1}{2} \ln \left(\frac{1 + \cos \alpha_\pm}{1 - \cos \alpha_\pm} \right). \quad (10)$$

Note that $0 \leq \alpha_\pm \leq \pi/2$ if $y_\pm \geq 0$, and $\pi/2 \leq \alpha_\pm \leq \pi$ if $y_\pm \leq 0$.

Let us analyze the scattering angle θ^* which determines the $q\bar{q} \rightarrow \tau^- \tau^+$ spin-correlation matrix in the c.m. frame.

¹Kinematic variables in the $\tau^- \tau^+$ c.m. frame are indicated with superscript *.

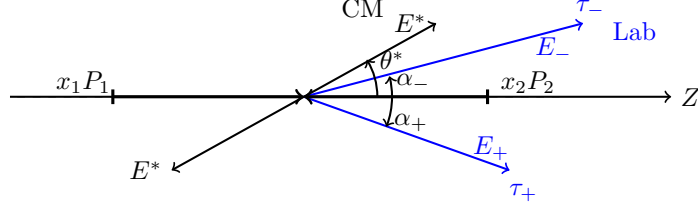


Figure 1: Configuration of τ^+ and τ^- momenta in lab and c.m. frames.

- If x_1 corresponds to quark and x_2 to antiquark, then θ^* is the angle between the quark and τ^- lepton. In the interval $0 \leq \theta^* \leq \pi$ the sign of $\sin \theta^*$ is always positive, while the sign of $\cos \theta^*$ depends on the sign of the rapidity y^* .
- If x_1 corresponds to antiquark and x_2 to quark, then one needs to change the angle $\theta^* \rightarrow \pi - \theta^*$ in the matrix $R_{i,j}^{(q\bar{q})}(M, \theta^*)$, and perform additional rotation on the latter (see further). The corresponding cross section is denoted below with “tilde”.

The cross section taking into account both possibilities is written in the form

$$\begin{aligned}
 \frac{d\sigma}{dY_Z dy^* dM^2} (pp \rightarrow \tau^- \tau^+ + \dots) &= \frac{x_1 x_2}{2 \cosh^2(y^*)} \quad (11) \\
 &\times \sum_{q=u,d,s,\dots} \left[F_q(x_1) F_{\bar{q}}(x_2) \frac{d\sigma}{dt} (q\bar{q} \rightarrow \tau^- \tau^+) \right. \\
 &\left. + F_{\bar{q}}(x_1) F_q(x_2) \frac{d\tilde{\sigma}}{dt} (q\bar{q} \rightarrow \tau^- \tau^+) \right].
 \end{aligned}$$

2.2 Kinematics for τ spin quantization frames

For the spin correlation matrix to be useful, we need to define all axes of the corresponding reference frames for τ^- and τ^+ separately.

Then, we can re-write and extend Eq. (11) to account for the decays of τ^\mp leptons to the final states $X^\mp \nu_\tau$

$$\begin{aligned}
 \frac{d\sigma}{dY_Z dy^* dM^2 d\Omega_- d\Omega_+} (pp \rightarrow X^- X^+ \nu_\tau \bar{\nu}_\tau + \dots) &= \frac{\beta x_1 x_2}{32\pi M^4 \cosh^2(y^*)} \quad (12) \\
 &\times \sum_{q=u,d,s,\dots} \left[F_q(x_1) F_{\bar{q}}(x_2) \sum_{i,j=1}^4 R_{i,j}^{(q\bar{q})}(M, \theta^*) h_i^- h_j^+ \right. \\
 &\left. + F_{\bar{q}}(x_1) F_q(x_2) \sum_{i,j=1}^4 \tilde{R}_{i,j}^{(q\bar{q})}(M, \pi - \theta^*) h_i^- h_j^+ \right],
 \end{aligned}$$

where Ω_- , Ω_+ are solid angles of the final hadrons X^- , X^+ . In Eq. (12) h_i^- and h_j^+ are the spin polarimetric vectors of τ^- and τ^+ decays, respectively, which depend on the τ -decay products momenta.

The first sum in the brackets of Eq. (12) corresponds to contribution where the laboratory \hat{z} axis corresponds to the direction of the incoming quark q . For the second part, the laboratory \hat{z} axis is along the direction of antiquark \bar{q} . Because we are interested in the spin correlations, and not in the unpolarized cross section, the second hard-scattering frame needs to be properly oriented. This results in

$$\tilde{R}_{i,j}^{(q\bar{q})}(M, \pi - \theta^*) \equiv \hat{O}_{z'}(\pi) R_{i,j}^{(q\bar{q})}(M, \pi - \theta^*) = \varepsilon_i \varepsilon_j R_{i,j}^{(q\bar{q})}(M, \pi - \theta^*), \quad (13)$$

where $\hat{O}_{z'}(\pi)$ is rotation around \hat{z}' axis by the angle π . Further, $\varepsilon_i = -1$ for $i = 1, 2$ and $\varepsilon_i = +1$ for $i = 3, 4$.

To calculate event weight we sum the spin-correlation coefficients in the $q\bar{q} \rightarrow \tau^- \tau^+$ process over the parton flavors

$$\begin{aligned} wt_{prod} wt_{spin} &= \sum_{i,j=1}^4 R_{i,j}^{(pp)} h_i^- h_j^+ \\ &= R_{44}^{(pp)} \left(1 + \sum_{i=1}^3 r_{i,4}^{(pp)} h_i^- + \sum_{j=1}^3 r_{4,j}^{(pp)} h_j^+ + \sum_{i,j=1}^3 r_{i,j}^{(pp)} h_i^- h_j^+ \right), \end{aligned} \quad (14)$$

where

$$\begin{aligned} R_{i,j}^{(pp)} &\equiv x_1 x_2 \sum_{q=u,d,s,\dots} \left[F_q(x_1) F_{\bar{q}}(x_2) R_{i,j}^{(q\bar{q})}(M, \theta^*) \right. \\ &\quad \left. + F_{\bar{q}}(x_1) F_q(x_2) \tilde{R}_{i,j}^{(q\bar{q})}(M, \pi - \theta^*) \right] \end{aligned} \quad (15)$$

for $i, j = 1, 2, 3, 4$, and define elements of effective proton-proton spin-correlation matrix $r_{i,j}^{(pp)}$ and τ^- (τ^+) polarization $r_{i,4}^{(pp)}$ ($r_{4,j}^{(pp)}$) in Eq. (14) as

$$r_{i,j}^{(pp)} = \frac{R_{i,j}^{(pp)}}{R_{44}^{(pp)}}, \quad r_{i,4}^{(pp)} = \frac{R_{i,4}^{(pp)}}{R_{44}^{(pp)}}, \quad r_{4,j}^{(pp)} = \frac{R_{4,j}^{(pp)}}{R_{44}^{(pp)}} \quad (i, j = 1, 2, 3). \quad (16)$$

These elements depend on the variables Y_Z , y^* and M^2 . We further omit superscript (pp) for brevity.

The definition of the anomalous magnetic $X(M^2)$ and electric $Y(M^2)$ dipole form-factors, and their relation to the corresponding weak dipole moments at $M = M_Z$ is given in [12]. Note that in the calculation only the linear in $X(M^2)$ and $Y(M^2)$ contributions are included, as one can expect their values to be very small. Indeed, the experiment ALEPH [14] determined the following constraints

$$\begin{aligned} |\text{Re}(\mu_\tau)|_{exp} &< 1.14 \times 10^{-3}, & |\text{Im}(\mu_\tau)|_{exp} &< 2.65 \times 10^{-3}, \\ |\text{Re}(d_\tau)|_{exp} &< 0.91 \times 10^{-3}, & |\text{Im}(d_\tau)|_{exp} &< 2.01 \times 10^{-3}, \end{aligned} \quad (17)$$

while the SM prediction [15] for the weak magnetic moment is ²

$$\mu_{\tau, SM} = -(2.10 + i 0.61) \times 10^{-6}. \quad (18)$$

The detailed definitions of axes of the τ reference frames are not necessary for the formula (14) phenomenology to be discussed. We will return to this point later, in fact, we will rely on the frames built from secondary decays momenta.

3 Numerical results on spin density matrix

In this section, we discuss numerical results on the spin-correlation matrix averaged over PDFs in Eqs. (15). The PDFs ‘‘MSTW 2008’’ from Ref. [16] are used in the calculation.

Let us start a discussion of the numerical results for the elements of the matrix in Eqs. (16). There are two interesting kinematic regimes. The first corresponds to the small rapidity of the τ -lepton pair, and the second corresponds to the situation, where the τ pair is strongly boosted. In the later case the quark is more probable to come from the first of the colliding protons. For example, from Table 1 and also from behavior of PDFs given in Fig. 2 it is clear, that at large rapidity $Y_Z = 4$ the parton carrying fraction x_1 of the proton momentum is usually the valence quark, while the other parton is the sea antiquark.

In the figures below, we choose the proton-proton energy $\sqrt{s} = 13.6$ TeV, the $\tau^- \tau^+$ pair invariant mass $M = M_Z$, and fix the total τ -pair rapidity Y_Z . To completely determine kinematics one needs to fix also the c.m. rapidity y^* . The latter is chosen to correspond to the c.m. angle $\theta^* = 60^\circ$. Values of kinematic variables for the three values $Y_Z = 0, 2, 4$ are shown in Table 1.

In Figs. 3, 4 and 5 we present dependence of the non-diagonal elements r_{12} , r_{13} , r_{23} , r_{14} and r_{24} on values of the real and imaginary parts of the weak anomalous magnetic and electric dipole moments X and Y , respectively. The diagonal elements of the spin-correlation matrix, r_{11} , r_{22} and r_{33} , are less sensitive to X and Y and are not shown.

The element r_{34} is equal to the longitudinal polarization of the τ^- lepton, and its value depends on the rapidity Y_Z due to the different composition of the parton flavors (an average in Eq. (15)). In particular, in the SM

$$\begin{aligned} r_{34} &= -0.150 & \text{for } Y_Z = 0, \\ r_{34} &= -0.386 & \text{for } Y_Z = 2, \\ r_{34} &= -0.725 & \text{for } Y_Z = 4, \end{aligned} \quad (19)$$

and r_{34} depends weakly on the anomalous dipole moments. For this reason, it is not shown in Figs. 3–5.

²Our dipole moments are related to μ_τ and d_τ via the relations: $X(M_Z^2) = \sin 2\theta_W \mu_\tau$, $Y(M_Z^2) = \sin 2\theta_W d_\tau$, where $\sin 2\theta_W \approx 0.843$ and θ_W is the weak mixing angle.

variable	$Y_Z = 0$	$Y_Z = 2$	$Y_Z = 4$
y^*	0.549306	0.549306	0.549306
y_-	0.549306	2.54931	4.54931
y_+	-0.549306	1.45069	3.45069
x_1	0.006705	0.049543	0.366079
x_2	0.006705	0.000907	0.000123
α_- (deg)	60	8.93556	1.21171
α_+ (deg)	120	26.3848	3.63404
θ^* (deg)	60	60	60
p_\perp (GeV)	39.4854	39.4854	39.4854
E_- (GeV)	45.5938	254.214	1867.21
E_+ (GeV)	45.5938	88.8516	622.961

Table 1: Rapidity y^* , rapidities of τ^- and τ^+ leptons y_- and y_+ , parton fractions x_1 , x_2 , angles α_- and α_+ of τ^- and τ^+ in lab frame, c.m. angle θ^* , transverse momentum p_\perp of τ leptons and their energies E_- , E_+ in lab frame.

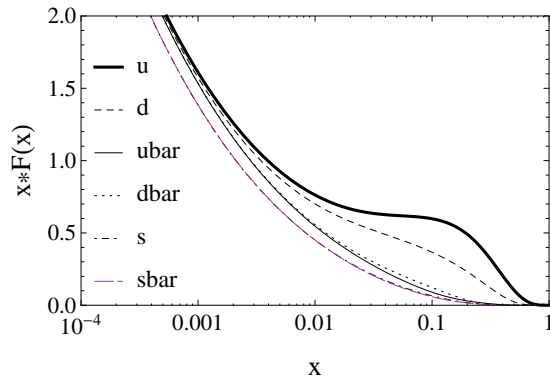


Figure 2: Parton distribution functions MSTW 2008 at the energy scale $Q = M_Z$.

One can see that some elements of $r_{i,j}$ and $r_{i,4}$ are sensitive to dipole moments. In particular, it is seen from Fig. 3 that r_{14} and r_{24} are sensitive to $\text{Re}(X)$ and $\text{Re}(Y)$, while r_{23} and r_{13} are sensitive to $\text{Im}(X)$ and $\text{Im}(Y)$. This may be convenient for separating magnetic and electric moment contributions, as well as their real and imaginary parts.

The pattern at larger rapidities in Figs. 4 and 5 becomes more complex, although sensitivity of $r_{i,j}$ to dipole moments is enhanced.

One can see that regimes of small and large (but still available for measurements at about $Y_Z = 2$) rapidity differ, but all regions preserve useful dependence on dipole moments, and thus can be useful for the development of

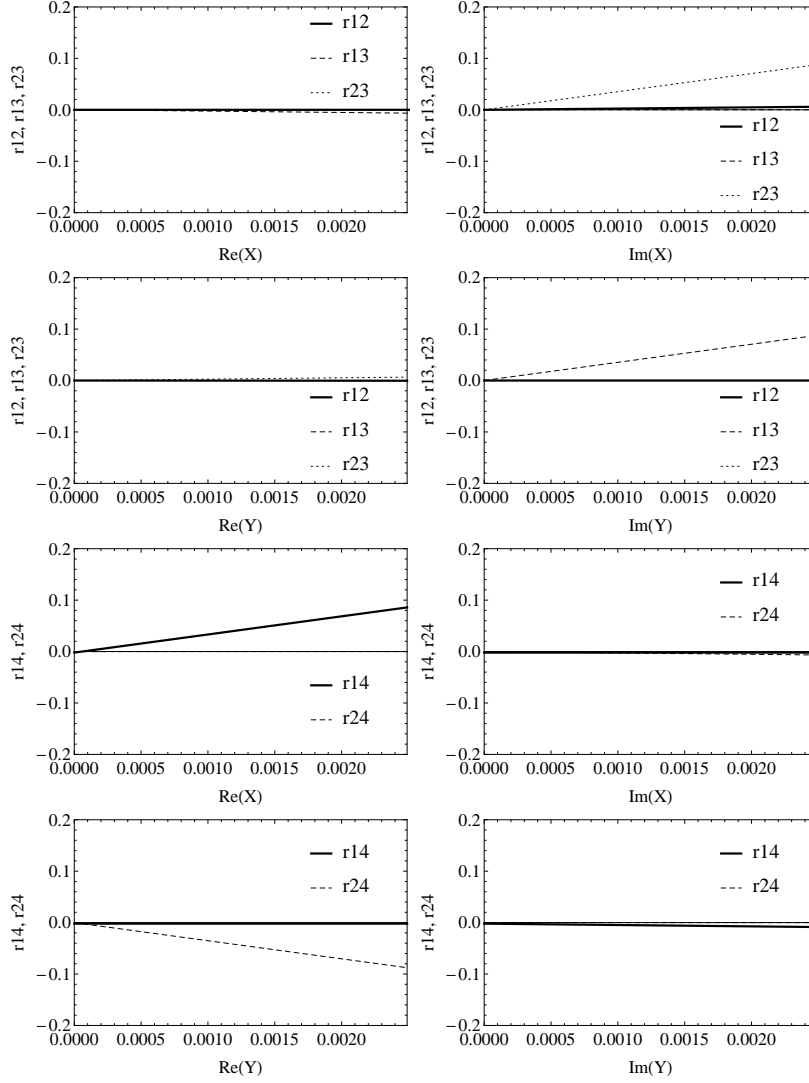


Figure 3: Dependence of $r_{i,j}$ on the real and imaginary parts of the weak magnetic and electric dipole moments. Proton-proton energy is 13.6 TeV, τ -pair invariant mass is equal to M_Z , Z -boson rapidity is $Y_Z = 0$ and c.m. angle is 60° . The contribution to the cross section of the quark with the momentum fraction x_1 (and correspondingly antiquark with fraction x_2) is 55.4%, and of the antiquark with fraction x_1 (and correspondingly quark with fraction x_2) – 44.6%. Elements $r_{i,j}$ which are not displayed in the figure are consistent with zero.

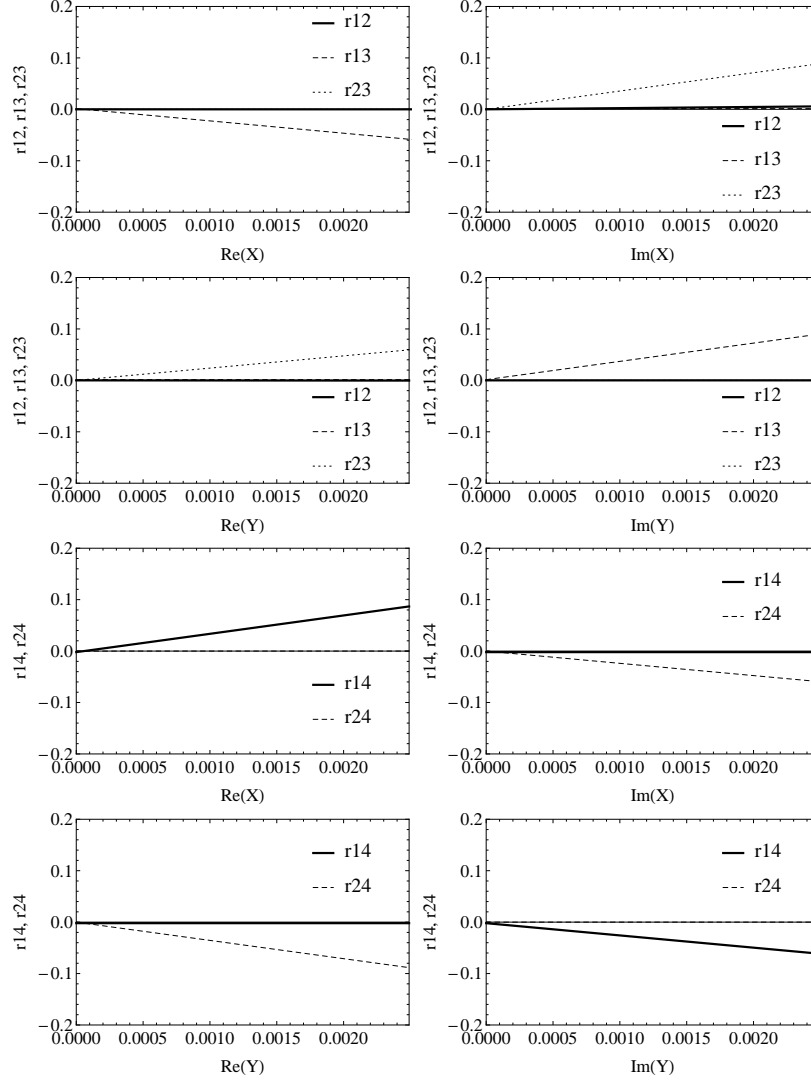


Figure 4: The same as in Fig. 3 but for rapidity $Y_Z = 2$. The contribution to the cross section of the quark with the momentum fraction x_1 (and correspondingly antiquark with fraction x_2) is 72.5%, and of the antiquark with fraction x_1 (and correspondingly quark with fraction x_2) – 27.5%.

observables. In the following Section we will concentrate on the r_{14} and r_{24} sensitivity to $\text{Re}(X)$ and $\text{Re}(Y)$.

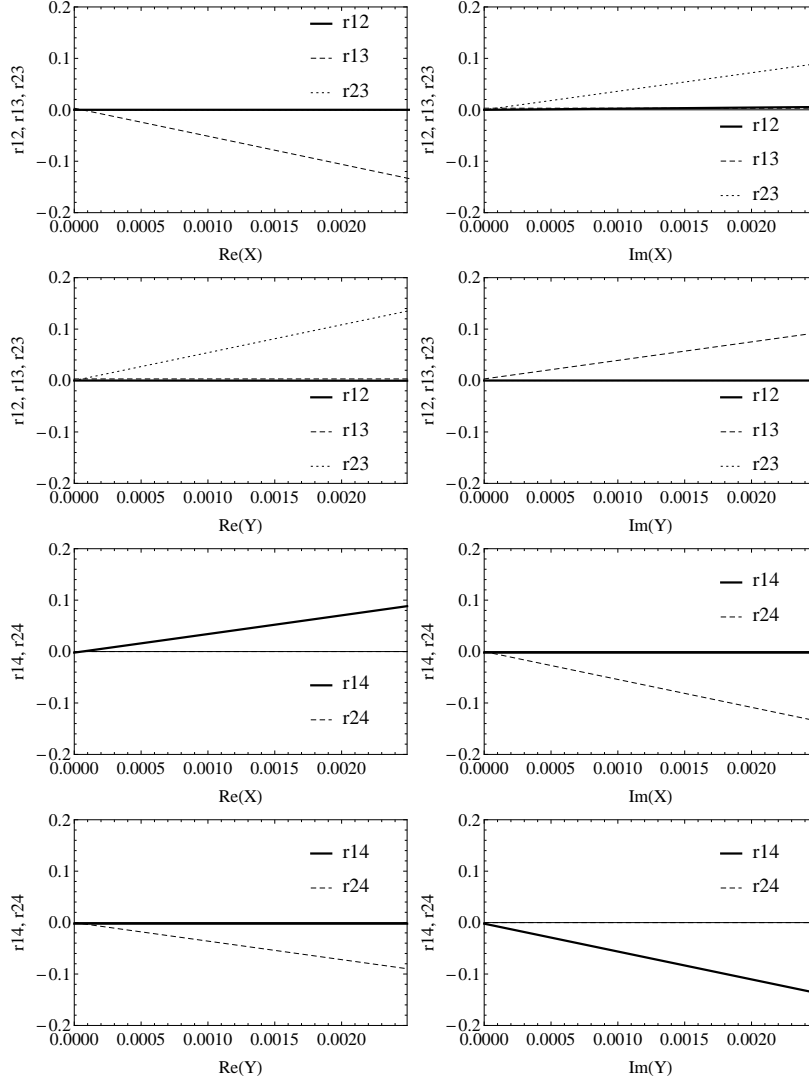


Figure 5: The same as in Fig. 3 but for rapidity $Y_Z = 4$. The contribution to the cross section of the quark with the momentum fraction x_1 (and correspondingly antiquark with fraction x_2) is 97.8%, and of the antiquark with fraction x_1 (and correspondingly quark with fraction x_2) – 2.2%.

4 Numerical results on sensitive observable

In the previous Section, we have investigated elements of the $r_{i,j}$ matrix. Now we can use that experience to search for one-dimensional distribution sensitive to

anomalous moments which can serve as the prototype for an observable, useful for the tests as well. Because of neutrinos escaping detections, and because the most sensitive to dipole moments turn out to be elements r_{14} , r_{24} , r_{13} and r_{23} , we use $\tau^\mp \rightarrow \pi^\mp \nu_\tau$ decay for its sensitivity to the longitudinal spin, and $\tau^\pm \rightarrow \rho^\pm \nu_\tau \rightarrow \pi^\pm \pi^0 \nu_\tau$ decay for its sensitivity to the transverse spin. In the pp collisions, reconstruction of τ momenta is difficult and we could only partly rely on experience of Ref. [12].

Our test observable was defined from the four momenta of the visible decay product system. This consists of acoplanarity angle ϕ between oriented half-planes built respectively on $\vec{p}_{beam1} \times (\vec{p}_{\pi^\pm} + \vec{p}_{\pi^0})$ and $\vec{p}_{beam1} \times \vec{p}_{\pi^\mp}$. Let us provide details of the ϕ angle definition. The *beam1* denotes the direction of the first beam ³.

As sensitivity observable, acoplanarity angle ϕ calculated in the rest frame of visible tau lepton decay products is used. This angle is defined as follows: first we define normal versors \vec{n}_1 to the plane spanned on the beam direction and π^\mp direction of $\tau^\mp \rightarrow \pi^\mp \nu_\tau$ decay, and \vec{n}_2 for plane spanned on π^\pm and π^0 directions for $\tau^\pm \rightarrow \rho^\pm \nu_\tau$. Acoplanarity angle is then calculated as arccos of $\vec{n}_1 \cdot \vec{n}_2$ scalar product, thus in $(0, \pi)$ range only. To extend the definition of acoplanarity to one of two oriented half-planes and to $(0, 2\pi)$ range, the scalar product of π^\mp from τ^\mp and \vec{n}_2 is used, if it is positive, we set acoplanarity angle equal to $2\pi - \phi$.

Such observable will still have negligible sensitivity to anomalous couplings. We need to split the sample into two parts according to the sign of the scalar product of versor \vec{n}_3 (normal to the plane spanned on the beam versor and \vec{n}_1 versor) and \vec{n}_2 . We denote them as **Region 1** and **Region 2**.

Fig. 6 shows the ratio of acoplanarity angle distribution for three settings of anomalous dipole moments to the SM predictions and for **Region 1** on the left-hand side, and **Region 2** on the right-hand side.

We have chosen for the plots $\text{Re}(X) = 2 \times 10^{-4}$, $\text{Re}(Y) = 2 \times 10^{-4}$ and imaginary parts of the dipole moments were set to zero, see Fig. 6. Sensitivity to dipole moments through the τ spin correlations could be demonstrated in semi-realistic condition of observable build from visible decay products of τ 's.

The sample used in the analysis has been generated using Pythia 8.2 Monte Carlo generator [17], with pp collision at 13.6 TeV c.m. energy and MSTW2008nmlo68cl.LHgrid parametrization of PDFs. The sample of 4×10^6 events of the hard process $q\bar{q} \rightarrow Z \rightarrow \tau^-\tau^+$ was generated with the invariant mass of τ -lepton pair restricted to the $M_Z \pm 0.5$ GeV range. Tau leptons were decayed with Tauola library [18] without spin correlations included, with one tau decaying into $\tau^\mp \rightarrow \pi^\mp \nu_\tau$ and second tau into $\tau^\pm \rightarrow \rho^\pm \nu_\tau \rightarrow \pi^\pm \pi^0 \nu_\tau$. Spin correlations were included with reweighting provided by **TauSpinner** package [10], to which formulas of [12] were implemented ⁴.

³Alternatively we have used also beam direction following z component of the visible system $\pi^\mp \pi^\pm \pi^0$ momentum.

⁴A comment on the orientation of reference frames is in place. One often interchanges the notations $\bar{q}q \rightarrow \tau^+\tau^-$ and $q\bar{q} \rightarrow \tau^-\tau^+$. This seemingly trivial order adjustment is of consequences. In particular for the reference frame of the c.m. system. This makes the

Spin weights were calculated for different models: the SM with $\text{Re}(X) = \text{Re}(Y) = 0.0$, and a few versions of anomalous moments included: (a) with $\text{Re}(X) = \text{Re}(Y) = 2 \times 10^{-4}$, (b) $\text{Re}(X) = 2 \times 10^{-4}$, $\text{Re}(Y) = 0$, (c) $\text{Re}(Y) = 2 \times 10^{-4}$, $\text{Re}(X) = 0$. These dipole couplings are smaller by about a factor of 10^{-3} with respect to the SM vector and axial-vector couplings, therefore their linear implementation into the differential cross section is reasonable. On the other hand, these dipole couplings are larger than the SM value (18) by a factor of 10^2 , so that the chosen values are sufficient to reflect the effect of NP.

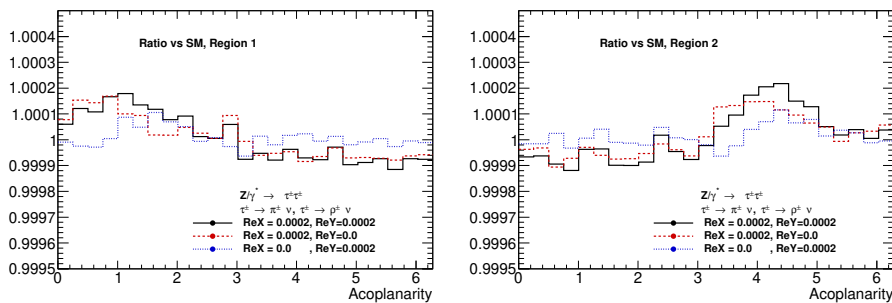


Figure 6: Ratio of acoplanarity angle ϕ distribution as defined in the text, with: (i) anomalous magnetic, (ii) electric, and (iii) simultaneously both magnetic and electric dipole moments included, to the distribution in which dipole moments were absent. Selection cut of **Region 1** (left plot) and of **Region 2** (right plot).

Fig. 6 shows the ratio of acoplanarity angle distribution with/without anomalous dipole moments. Distributions in **Region 1** and **Region 2** are shown separately. One can observe the effect on the shape of distribution on the level of 10^{-4} in the **Region 1** and **Region 2** for the acoplanarity angles $(0, \pi)$ and $(\pi, 2\pi)$, respectively.

As the dipole moments are introduced at the linear level through the interference with the SM amplitudes, their effect shown in Fig. 6 can be obtained for other values of $X(M_Z^2)$ and $Y(M_Z^2)$ by a simple rescaling. Note also, that because of weighted event samples, the statistical error affects the NP effect alone and not from the difference of the independently obtained results for distinct anomalous coupling values. Therefore, the obtained numerical results are meaningful even though a sample of only $N = 4 \times 10^6$ events was used. That is why, statistical error on NP effect is substantially smaller than $1/\sqrt{N} = 0.5 \times 10^{-3}$

difference if one chooses the axis \hat{z}' along the τ^- momentum (as in Section 2), or takes $\bar{q}q \rightarrow \tau^+\tau^-$ and directs \hat{z}' along the τ^+ momentum, as used in conventions of **TauSpinner** and also **KKMC** MC. Both descriptions are of course equivalent, although to connect different conventions, rotation around the axis \hat{y}' by the angle π may be needed as well as interchange of indices i, j in the spin-correlation matrix $R_{i,j}^{(qq)}$. This point was already addressed in Ref. [12], see there Section II footnote 1 and Subsection IV.A, in context of $e^+e^- \rightarrow \tau^+\tau^-$ production.

expected for the compared distribution features.

In future we can use π^\mp energy, or equivalent variable to explore anomalous moment dependence due to elements r_{13} and r_{23} which are sensitive to imaginary parts of $X(M_Z^2)$ and $Y(M_Z^2)$.

5 Summary

We have investigated the possibility of using the spin effects of the Drell-Yan τ -pair production and decay in the LHC conditions. For that purpose we constructed observables sensitive to the presence/absence of anomalous dipole moments of the τ -lepton interaction. To simplify the task we have concentrated on couplings to the Z boson. Interaction with virtual photons is potentially more involved as no constraint of the Z peak can be used. The couplings to virtual photons can be measured in the Belle experiments, for relatively low τ -pair virtuality though. For higher virtuality more complex evaluation of experimental cuts than presented here, would be needed. We leave it to the forthcoming work, preferably by the experiments themselves as discussion of experimental cuts will be of much greater importance.

We expect that our observable, demonstrating the sensitivity of spin-dependent observables to anomalous dipole moments, is primarily for the program tests. In final applications, Machine Learning (ML) techniques will be far more suitable, but even in those cases, idealized optimal-like variables may be helpful to prepare the primary set of variables used as input for ML algorithm training. Such variables may help study experimental ambiguities too. The demonstrated extension of `TauSpinner` algorithm may be helpful in such projects.

Acknowledgment

Numerical calculations were partially performed at the PLGrid Infrastructure of the Academic Computer Centre CYFRONET AGH in Krakow, Poland. This research was funded in part by National Science Centre, Poland, grant No. 2023/50/A/ST2/00224.

References

- [1] Friedrich Jegerlehner. *The Anomalous Magnetic Moment of the Muon*, volume 274. Springer, Cham, 2017.
- [2] T. Aoyama et al. The anomalous magnetic moment of the muon in the Standard Model. *Phys. Rept.*, 887:1–166, 2020.
- [3] B. Abi et al. Measurement of the Positive Muon Anomalous Magnetic Moment to 0.46 ppm. *Phys. Rev. Lett.*, 126(14):141801, 2021.

- [4] T. Albahri et al. Measurement of the anomalous precession frequency of the muon in the Fermilab Muon g-2 Experiment. *Phys. Rev. D*, 103(7):072002, 2021.
- [5] D. P. Aguillard et al. Measurement of the Positive Muon Anomalous Magnetic Moment to 0.20 ppm. *Phys. Rev. Lett.*, 131(16):161802, 2023.
- [6] Georges Aad et al. Observation of the $\gamma\gamma \rightarrow \tau\tau$ Process in $Pb+Pb$ Collisions and Constraints on the τ -Lepton Anomalous Magnetic Moment with the ATLAS Detector. *Phys. Rev. Lett.*, 131(15):151802, 2023.
- [7] Armen Tumasyan et al. Observation of τ lepton pair production in ultraperipheral lead-lead collisions at $\sqrt{s_{NN}} = 5.02$ TeV. *Phys. Rev. Lett.*, 131:151803, 2023.
- [8] CMS Collaboration. Observation of $\gamma\gamma \rightarrow \tau\tau$ in proton-proton collisions and limits on the anomalous electromagnetic moments of the τ lepton, June 2024. arXiv:2406.03975.
- [9] E. Richter-Was and Z. Was. Documentation of *TauSpinner* approach for electroweak corrections in LHC $Z \rightarrow \ell\ell$ observables. *Eur. Phys. J. C*, 79(6):480, 2019.
- [10] T. Przedzinski, E. Richter-Was, and Z. Was. Documentation of *TauSpinner* algorithms: program for simulating spin effects in τ -lepton production at LHC. *Eur. Phys. J. C*, 79(2):91, 2019.
- [11] E. Richter-Was and Z. Was. Adequacy of Effective Born for electroweak effects and TauSpinner algorithms for high energy physics simulated samples. *Eur. Phys. J. Plus*, 137(1):95, 2022.
- [12] Sw. Banerjee, A. Yu. Korchin, E. Richter-Was, and Z. Was. Electron-positron, parton-parton, and photon-photon production of τ -lepton pairs: Anomalous magnetic and electric dipole moments spin effects. *Phys. Rev. D*, 109(1):013002, 2024.
- [13] Michael E. Peskin and Daniel V. Schroeder. *An Introduction to quantum field theory*. Addison-Wesley, Reading, USA, 1995.
- [14] A. Heister et al. Search for anomalous weak dipole moments of the tau lepton. *Eur. Phys. J. C*, 30:291–304, 2003.
- [15] J. Bernabeu, G. A. Gonzalez-Sprinberg, M. Tung, and J. Vidal. The Tau weak magnetic dipole moment. *Nucl. Phys. B*, 436:474–486, 1995.
- [16] A. D. Martin, W. J. Stirling, R. S. Thorne, and G. Watt. Parton distributions for the LHC. *Eur. Phys. J. C*, 63:189–285, 2009.

- [17] Torbjörn Sjöstrand, Stefan Ask, Jesper R. Christiansen, Richard Corke, Nishita Desai, Philip Ilten, Stephen Mrenna, Stefan Prestel, Christine O. Rasmussen, and Peter Z. Skands. An introduction to PYTHIA 8.2. *Comput. Phys. Commun.*, 191:159–177, 2015.
- [18] N. Davidson, G. Nanava, T. Przedzinski, E. Richter-Was, and Z. Was. Universal Interface of TAUOLA Technical and Physics Documentation. *Comput. Phys. Commun.*, 183:821–843, 2012.